

# Technical Notes

TECHNICAL NOTES are short manuscripts describing new developments or important results of a preliminary nature. These Notes cannot exceed 6 manuscript pages and 3 figures; a page of text may be substituted for a figure and vice versa. After informal review by the editors, they may be published within a few months of the date of receipt. Style requirements are the same as for regular contributions (see inside back cover).

## Attenuating the Transverse Edge Effect in MHD Generators

Alexander Yakhot\*

Ben Gurion University of the Negev, Beersheva, Israel  
and

Alexei Levin†  
Technion, Haifa, Israel

### Introduction

THE longitudinal edge effect associated with a sharp drop in the magnetic field when entering and leaving the channel of an MHD generator results in the formation of closed current loops (Fig. 1a), which reduce the net generator output, increase Joule losses, and reduce the generator efficiency. It was suggested by Sutton<sup>1</sup> that the longitudinal edge effect be attenuated by placing nonconducting partitions at the inlet and exit of the electrode zone.

A specific inhomogeneity of the electric current, the so-called "transverse edge effect," also arises in the channel cross section when, as a result of nonuniformity of the velocity in the direction of the magnetic field, a part of the current forms a closed loop over the boundary layers near nonconducting walls (Fig. 1b).

We suggest in this study that nonconducting baffles, parallel to the magnetic field and adjoining the insulated walls, be placed in the electrode region of the generator. By analogy with the partitions employed by Sutton,<sup>1</sup> such a placement of baffles just will attenuate the shunting currents flowing along boundary layers at the insulated walls of the channel (Fig. 1b).

### Problem Statement and Solution

We consider a rectangular channel with walls  $x = \pm a$  insulated and walls  $y = \pm h$  serving as electrodes. An electrically conducting fluid with constant conductivity  $\sigma$  and specified velocity  $V = [0, 0, -V_0 u_0(x)]$  flows in the channel. Here  $V_0$  is some characteristic velocity,  $u_0(x)$  is a dimensionless function, even in  $x$  and such that  $u_0(\pm a) = 0$  and

$$\langle u_0(x) \rangle = \frac{1}{2a} \int_{-a}^a u_0(x) dx = 1$$

The channel is placed in a constant magnetic field  $B = (B_0, 0, 0)$ . Nonconducting baffles  $\alpha a < |x| < a$ ,  $0 \leq \alpha \leq 1$  are placed in the plane  $y = 0$  (Fig. 1b). The channel is assumed to be infinitely long and all the variables are taken to be independent of the coordinates of flow direction.

Transforming to dimensionless quantities, we write Ohm's law for the density of the electric current projected on the coordinate axes

$$j_x = -\partial\phi/\partial x, \quad j_y = -\partial\phi/\partial y - u_0(x) \quad (1)$$

Received Nov. 11, 1977; revision received June 26, 1978. Copyright © 1978 by Alexander Yakhot with release to the American Institute of Aeronautics and Astronautics, Inc., to publish in all forms.

Index category: MHD.

\*Lecturer, Dept. of Mechanical Engineering.

†Lecturer, Mathematics Dept.

Here the channel height  $h$ ,  $\sigma V_0 B_0$ , and  $V_0 B_0 h$  are, respectively, the reference quantities for the  $x$  and  $y$  coordinates, current density  $j$  and electric potential  $\phi$ .

Since  $\text{div} j = 0$ , the electric potential  $\phi(x, y)$  satisfies the Laplace equation with boundary conditions:

$$\frac{\partial\phi}{\partial x} = 0 \text{ at } y = \pm 1, \quad |x| < a/h \quad (2)$$

$$\frac{\partial\phi}{\partial x} = 0 \text{ at } x = \pm a/h, \quad |y| < 1 \quad (3)$$

$$\frac{\partial\phi}{\partial y} = -u_0(x) \text{ at } \alpha a/h < |x| < a/h \quad (4)$$

Electric potential  $\phi(x, y)$  is a harmonic function, odd in  $y$  and, consequently, it suffices to solve the problem for the top half of the channel. We conformally map the top half of the channel onto the top half plane  $w = u + iv$  (Fig. 2). Such a conformal transformation is implemented by the elliptical integral<sup>2</sup>

$$z = C \int_0^w \frac{dt}{[(1-t^2)(1-k^2 t^2)]^{1/2}} \quad (5)$$

For a given value of ratio  $a/h$  the constants  $C$  and  $k$  can be found from equations  $a/h = K(k)/K(k')$ ,  $1 = CK(k')$ . Here

$$K(k) = \int_0^1 \frac{dt}{[(1-t^2)(1-k^2 t^2)]^{1/2}}$$

is a complete elliptical integral of the first kind and  $k^2 + k'^2 = 1$ ,  $0 < k < 1$ . The constant  $\alpha$  specifies the size of the baffle and the value of  $q$  which "is responsible" for the size of the baffle in the  $w$  plane is found from correspondence of points  $Q \rightarrow q$

$$\frac{\alpha a}{h} = C \int_0^q \frac{dt}{[(1-t^2)(1-k^2 t^2)]^{1/2}}, \quad 0 < q < 1 \quad (6)$$

Harmonic function  $\phi(x, y)$  under transformation (5) becomes the harmonic function  $\tilde{\phi}(u, v)$  satisfying the following boundary conditions

$$\frac{\partial\tilde{\phi}}{\partial u} = 0 \text{ at } |u| < q, \quad v = 0 \quad (7)$$

$$\frac{\partial\tilde{\phi}}{\partial v} = -\tilde{u}_0 \cdot \frac{C}{[(1-u^2)(1-k^2 u^2)]^{1/2}} \text{ at } q < |u| < 1, \quad v = 0 \quad (8a)$$

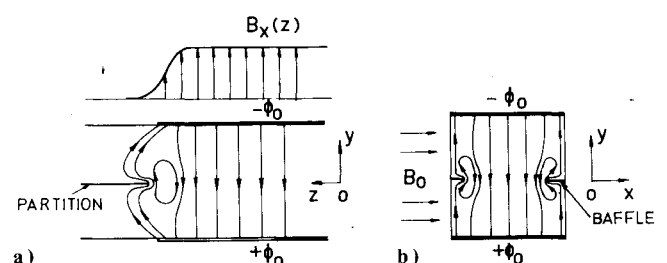


Fig. 1 a) Longitudinal edge effect; b) transverse edge effect.

$$\frac{\partial \bar{\phi}}{\partial v} = 0 \text{ at } I < |u| < I/k, \quad v=0 \quad (8b)$$

$$\frac{\partial \bar{\phi}}{\partial u} = 0 \text{ at } |u| > I/k, \quad v=0 \quad (9)$$

Here function  $\bar{u}_0(u)$  is the image of function  $u_0(x)$  in half plane  $\text{Im} w > 0$ ,  $\bar{u}_0(u) = u_0[x(u)]$  and function  $x(u)$  is found from Eq. (5).

We now construct the analytic function  $\partial \bar{\phi} / \partial v + i \partial \bar{\phi} / \partial u$ . The task of finding harmonic function  $\bar{\phi}(u, v)$  now reduces to a known boundary-value problem on finding an analytic function in the top half plane, when the real axis is subdivided into segments, at which values of the real and imaginary parts of the analytic function are specified in sequence. The solution of this problem was found by Keldysh and Sedov,<sup>3</sup> and for boundary conditions (7-9) has the form

$$\begin{aligned} \partial \bar{\phi} / \partial v + i \partial \bar{\phi} / \partial u = & \frac{I}{\pi g(w)} \left[ \int_{-1}^{-q} \frac{\partial \bar{\phi} / \partial v \cdot g_1(t)}{t-w} dt \right. \\ & \left. + \int_q^I \frac{\partial \bar{\phi} / \partial v \cdot g_2(t)}{t-w} dt \right] + h(w) \end{aligned} \quad (10)$$

where

$$g_1(t) = \left( \frac{|t| - q}{|t| + q} \cdot \frac{I/k + |t|}{I/k - |t|} \right)^{1/2}, \quad g_2(t) = \left( \frac{t+q}{t-q} \cdot \frac{I/k - t}{I/k + t} \right)^{1/2}$$

$$g(w) = \left[ \frac{(w+q) \cdot (w-I/k)}{(w-q) \cdot (w+I/k)} \right]^{1/2}$$

$$h(w) = \frac{\gamma_0}{[(w^2 - q^2)(w^2 - I/k^2)]^{1/2}}$$

Real constant  $\gamma_0$  should be determined from conditions of the specified load circuit; this will be discussed below.

Equation (10) yields the general solution of the problem of distribution of the electric potential in a channel with nonconducting baffles.

### Current and Potential Difference

We designate the potential of the upper electrode by  $-\phi_0$  and that of the lower electrode by  $+\phi_0$ . Let us calculate the potential difference between points  $Q$  and  $N$  (Fig. 2):

$$\int_Q^N d\phi = -\phi_0 = \int_{QBN} d\phi = \int_{QBN} \frac{\partial \bar{\phi}}{\partial u} du \quad (11)$$

Using Eqs. (10) and (11), we obtain an expression for the electrode potential  $\phi_0$ :

$$\phi_0 = I_{1q} + \gamma_0 k K'(kq) \quad (12)$$

where

$$\begin{aligned} I_{1q} = & \frac{I}{\pi} \int_q^{I/k} \left( \frac{u-q}{u+q} \cdot \frac{I/k+u}{I/k-u} \right)^{1/2} \left[ \int_q^I \frac{\partial \bar{\phi} / \partial v \cdot g_2(t)}{t-u} dt \right. \\ & \left. - \int_q^I \frac{\partial \bar{\phi} / \partial v \cdot I/g_2(t)}{t+u} dt \right] du \end{aligned}$$

When the generator operates at a specified potential difference  $2\phi_0$  between the electrodes, Eq. (12) serves for finding the constant  $\gamma_0$ .

We calculate the load current

$$I = -2 \int_0^{\alpha a/h} j_y dx = 2 \int_0^q \frac{\partial \bar{\phi}}{\partial v} du + u_{0\alpha} \quad (13)$$

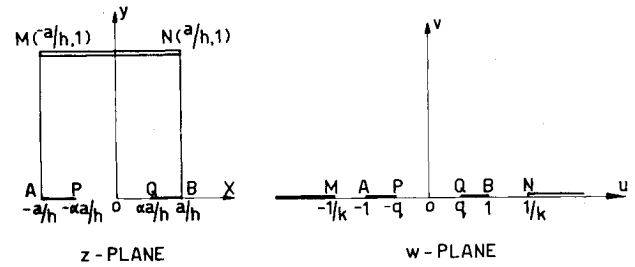


Fig. 2 Conformal mapping of a region onto the upper half plane.

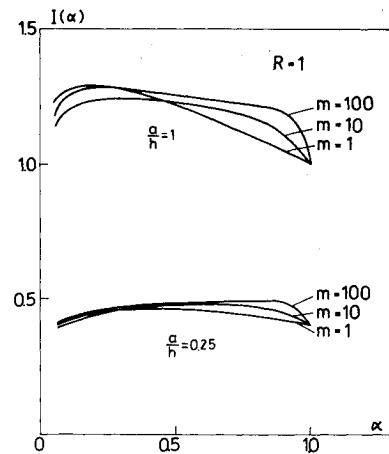


Fig. 3 Plot of  $I(\alpha)$  for a specified load resistance ( $R = 1$ ).

where

$$u_{0\alpha} = 2 \int_0^{\alpha a/h} u_0(x) dx$$

From Eqs. (10) and (13) we find expression for the load current

$$I = 2[I_{2q} - \gamma_0 k K(kq)] + u_{0\alpha} \quad (14)$$

where

$$\begin{aligned} I_{2q} = & \frac{I}{\pi} \int_0^q \left( \frac{q-u}{q+u} \cdot \frac{I/k+u}{I/k-u} \right)^{1/2} \left[ \int_q^I \frac{\partial \bar{\phi} / \partial v \cdot g_2(t)}{t-u} dt \right. \\ & \left. - \int_q^I \frac{\partial \bar{\phi} / \partial v \cdot I/g_2(t)}{t+u} dt \right] du \end{aligned}$$

When the electrodes are interconnected through an external resistance  $R$ , we have  $2\phi_0 = IR$  and obtain the expression

$$I_{1q} + \gamma_0 k K'(kq) = [I_{2q} - \gamma_0 k K(kq) + u_{0\alpha}/2]R \quad (15)$$

which, for a given load resistance  $R$ , serves for determining constant  $\gamma_0$ .

### Results of Calculations

The net current is a function of several parameters such as the ratio of channel walls ( $a/h$ ), size of nonconducting baffles ( $\alpha$ ), electrode potential ( $\phi_0$ ), or load resistance ( $R$ ) and also the velocity distribution. It is hence desirable to show in general form that the placement of nonconducting baffles in the channel increases the current output. For this purpose, it was shown by examining the asymptotic behavior of Eq. (14) for small baffles ( $\alpha \approx 1$ , meaning also  $q \approx 1$ ) that the expansion of Eq. (14) in power series in  $(1 - \alpha)$  is

$$I = I_0 + r^2(1 - \alpha) + O(1 - \alpha)^2 \quad (16)$$

Here  $I_0$  is load current when there are no baffles. When the potential difference is specified,  $I_0 = 2a/h(1 - \phi_0)$ , and when the load resistance  $R$  is given,  $I_0 = 2a/(h + aR)$ . Since in Eq. (16) the coefficient of  $(1 - \alpha)$  is positive, this means that the placing of baffles increases the net current.

In our calculations, the velocity distribution  $u_0(x)$  was expressed as

$$u_0(x) = m \frac{\cosh m - \cosh(mxh/a)}{m \cosh m - \sinh m}$$

and when parameter  $m$  goes from zero to infinity the distribution varies from the parabolic (Poiseuille distribution) to the homogeneous.

Figure 3 depicts calculated curves of current  $I$  as a function of size  $\alpha$  of the baffles. At  $\alpha = 0$  (the channel is completely blocked by the baffles, Fig. 2)  $I(\alpha = 0) = 0$ , however, the decrease in the current to zero with increase of baffle size is very slow. Since  $I(\alpha = 0) = 0$  and Eq. (16) is fulfilled at  $\alpha \approx 1$ , curves  $I(\alpha)$  have maxima. However, calculations show that, as  $m$  is increased, whereupon the velocity distribution becomes fuller, which corresponds to the case of a real MHD generator, the curve of  $I(\alpha)$  becomes flat without a sharply expressed peak. The latter fact allows the conclusion that in order to increase the net current it suffices to place small baffles. This is important, since it can be expected that the additional friction produced by placing these rather small baffles will not be so high as to significantly lessen the benefit of suppression of current flow reversal.

### Acknowledgment

This work was supported in part by the Office of Naval Research, U.S.A., under grant N00014-77-G-0034. The authors wish to thank H. Branover for discussion of their work and D. Michelson for performing the computations.

### References

- <sup>1</sup>Sutton, G. W., "Design Considerations of a Magnetohydrodynamic Electrical Power Generator," *Vistas Astronautics*, Vol. 3, SPE, New York, 1960, pp. 53-64.
- <sup>2</sup>Carrier, G., Krook, M., and Pearson, C., *Functions of a Complex Variable*, McGraw-Hill, N.Y., 1966.
- <sup>3</sup>Keldysh, M. V. and Sedov, L. I., "Effective Solution of some Boundary Value Problems for Harmonic Functions," *Doklady Akademii Nauk SSSR*, Vol. 16, No. 1, 1937, pp. 7-10.

## Finite Deformation of Anisotropic Plastic Rotating Disks

William W. Feng\*

University of California, Livermore, Calif.

### Introduction

MOST rolled sheet metals exhibit variations of yield stress and stress-strain relations with orientation, while the sheet remains approximately isotropic in its plane. This phenomenon was verified experimentally by Lilet and Wybo.<sup>1</sup> Constitutive equations for anisotropic plastic materials that harden according to a power law were developed by Hill.<sup>2</sup> The anisotropic property of the material is measured by a strain-ratio parameter that is defined on the

Received Jan. 3, 1978. This paper is declared a work of the U.S. Government and therefore is in the public domain.

Index categories: Materials, Properties of; Analytical and Numerical Methods.

\*Mechanical Engineer, Lawrence Livermore Laboratory.

basis of a uniaxial test as the ratio of the transverse plastic strain in the plane of the sheet to the plastic strain through the thickness. The strain hardening property is characterized by a constant that is the exponent of a power law relating the effective stress and strain. These constitutive equations and their influence on drawability of the degree of anisotropy and on the strain hardening characteristics have been studied by Budiansky and Wang.<sup>3</sup> Yang<sup>4</sup> has analyzed the stress concentration of circular sheets with imperfections using the same equations. In this Note, these equations are used to solve the nonlinear problem of rotating disks. The rotating disks exhibit anisotropic properties in planes other than their own. The material properties in the rotating plane are assumed to be isotropic; therefore, the axisymmetric rotating disk before deformation remains axisymmetric after deformation.

In the formulation and numerical calculations, large strains and finite deformations are considered. The formulation is similar to that used by Feng<sup>5</sup> in studying hyperelastic rubber disks under various loadings. The strains in the radial and circumferential directions are used as two dependent variables. The governing equations are reduced to two coupled first-order ordinary differential equations with explicit derivatives, and further reduced with the boundary conditions, to dimensionless forms. The equations with their appropriate boundary conditions can be solved by any numerical integration method. We have also introduced an efficient numerical method that eliminates the iteration scheme to satisfy the governing equations and the boundary conditions. Stress and strain distributions for a solid rotating disk are also included.

The results obtained in this paper can be applied directly to the study of the mechanics of flywheels. The formulation and numerical method can be extended to the whole class of axisymmetric plane-stress and axisymmetric membrane problems.

### Formulation

A rotating disk of anisotropic plastic material before and after deformation is shown in Fig. 1. A point  $p$  on the undeformed disk can be described by the undeformed polar coordinates  $(r, \theta)$ . Point  $p$  is deformed to point  $P$  and can be described by the deformed polar coordinates  $(R, \Theta)$ . For the axisymmetric problems,  $\Theta = \theta$  and  $R$  is an unknown function of  $r$ . In the analysis, the disk is assumed to be thin and the plane-stress problem leads to a good approximation.

The strain in the radial, tangential, and normal directions are defined respectively as

$$\epsilon_r = \ln(dR/dr) \quad \epsilon_\theta = \ln(R/r) \quad \epsilon_z = \ln(H/h) \quad (1)$$

where  $H$  is the thickness of the deformed disk and  $h$  (a constant in this analysis) is the thickness of the undeformed disk.

The total stress-strain relations derived from Hill's<sup>2</sup> incremental relation for anisotropic plasticity are

$$\epsilon_r = \frac{\epsilon}{\sigma} \left[ \sigma_r - \frac{\Gamma}{1+\Gamma} \sigma_\theta \right]$$

Fig. 1 Coordinates for a rotating disk.

